Generation of optical vortex array with transformation of standing-wave Laguerre-Gaussian mode

Y. C. Lin,[1] T. H. Lu,[2] K. F. Huang,[1] and Y. F. Chen[1,*]

[1]*Department of Electrophysics, National Chiao Tung University, Hsinchu, Taiwan*
[2]*Department of Physics, National Taiwan Normal University, Taipei, Taiwan*
**yfchen@cc.nctu.edu.tw*

Abstract: We develop a novel method of creating optical vortex array by the conversion of a standing-wave Laguerre-Gaussian (LG) mode. Theoretically, by employing the transformational relation, the standing-wave LG mode is verified to be transformed from a pair of crisscrossed Hermite-Gaussian (HG) modes, embedded with optical vortex array, consists of a $TEM_{n,m}$ mode and a $TEM_{m,n}$ mode. Due to close correspondence between the transformational relation and the mode conversion of astigmatic lenses, we successfully generate the optical vortex array by transforming a standing-wave LG mode into the crisscrossed HG modes via a $\pi/2$ cylindrical lens mode converter. The investigation may provide useful insight in the study of the vortex light beam and its further applications.

OCIS codes: (140.4480) Lasers, diode-pumped; (030.4070) Modes; (050.4865) Optical vortices; (350.5030) Phase.

References and links

1. K. T. Gahagan and G. A. Swartzlander, Jr., "Optical vortex trapping of particles," Opt. Lett. **21**(11), 827–829 (1996).
2. M. S. Soskin and M. V. Vasnetsov, "Singular Optics," Prog. Opt. **42**, 219–276 (2001).
3. N. B. Simpson, K. Dholakia, L. Allen, and M. J. Padgett, "Mechanical equivalence of spin and orbital angular momentum of light: an optical spanner," Opt. Lett. **22**(1), 52–54 (1997).
4. H. Adachi, S. Akahoshi, and K. Miyakawa, "Orbital motion of spherical microparticles trapped in diffraction patterns of circularly polarized light," Phys. Rev. A **75**(6), 063409 (2007).
5. A. Mair, A. Vaziri, G. Weihs, and A. Zeilinger, "Entanglement of the orbital angular momentum states of photons," Nature **412**(6844), 313–316 (2001).
6. L. Allen, M. W. Beijersbergen, R. J. C. Spreeuw, and J. P. Woerdman, "Orbital angular momentum of light and the transformation of Laguerre-Gaussian laser modes," Phys. Rev. A **45**(11), 8185–8189 (1992).
7. P. Senthilkumaran, "Optical phase singularities in detection of laser beam collimation," Appl. Opt. **42**(31), 6314–6320 (2003).
8. G. Gibson, J. Courtial, M. J. Padgett, M. Vasnetsov, V. Pas'ko, S. Barnett, and S. Franke-Arnold, "Free-space information transfer using light beams carrying orbital angular momentum," Opt. Express **12**(22), 5448–5456 (2004).
9. K. Crabtree, J. A. Davis, and I. Moreno, "Optical processing with vortex-producing lenses," Appl. Opt. **43**(6), 1360–1367 (2004).
10. K. Dholakia, N. B. Simpson, M. J. Padgett, and L. Allen, "Second-harmonic generation and the orbital angular momentum of light," Phys. Rev. A **54**(5), R3742–R3745 (1996).
11. M. W. Beijersbergen, L. Allen, H. Vanderveen, and J. P. Woerdman, "Astigmatic laser mode converters and transfer of orbital angular momentum," Opt. Commun. **96**(1-3), 123–132 (1993).
12. M. W. Beijersbergen, R. P. C. Coerwinkel, M. Kristensen, and J. P. Woerdman, "Helical-wavefront laser beams produced with a spiral phaseplate," Opt. Commun. **112**(5-6), 321–327 (1994).
13. N. R. Heckenberg, R. McDuff, C. P. Smith, and A. G. White, "Generation of optical phase singularities by computer-generated holograms," Opt. Lett. **17**(3), 221–233 (1992).
14. Y. Izdebskaya, V. Shvedov, and A. Volyar, "Generation of higher-order optical vortices by a dielectric wedge," Opt. Lett. **30**(18), 2472–2474 (2005).
15. G. Nienhuis and L. Allen, "Paraxial wave optics and harmonic oscillators," Phys. Rev. A **48**(1), 656–665 (1993).
16. E. Abramochkin and V. Volostnikov, "Beam transformation and nontransformed beams," Opt. Commun. **83**(1-2), 123–135 (1991).

#144024 - $15.00 USD Received 16 Mar 2011; revised 29 Apr 2011; accepted 8 May 2011; published 10 May 2011

17. Y. F. Chen, Y. C. Lin, K. F. Huang, and T. H. Lu, "Spatial transformation of coherent optical waves with orbital morphologies," Phys. Rev. A **82**(4), 043801 (2010).
18. S. Vyas and P. Senthilkumaran, "Interferometric optical vortex array generator," Appl. Opt. **46**(15), 2893–2898 (2007).
19. K. O'Holleran, M. J. Padgett, and M. R. Dennis, "Topology of optical vortex lines formed by the interference of three, four, and five plane waves," Opt. Express **14**(7), 3039–3044 (2006).
20. K. Otsuka and S. C. Chu, "Generation of vortex array beams from a thin-slice solid-state laser with shaped wide-aperture laser-diode pumping," Opt. Lett. **34**(1), 10–12 (2009).
21. J. Masajada, "Small-angle rotations measurement using optical vortex interferometer," Opt. Commun. **239**(4-6), 373–381 (2004).
22. M. D. Levenson, T. J. Ebihara, G. Dai, Y. Morikawa, N. Hayashi, and S. M. Tan, "Optical vortex mask via levels," J. Microlithogr. Microfabr. Microsyst. **3**(2), 293–304 (2004).
23. K. Ladavac and D. G. Grier, "Microoptomechanical pumps assembled and driven by holographic optical vortex arrays," Opt. Express **12**(6), 1144–1149 (2004).
24. G. H. Kim, J. H. Jeon, Y. C. Noh, K. H. Ko, H. J. Moon, J. H. Lee, and J. S. Chang, "An array of phase singularities in a self-defocusing medium," Opt. Commun. **147**(1-3), 131–137 (1998).
25. G. Grynberg, A. Maître, and A. Petrossian, "Flowerlike patterns generated by a laser beam transmitted through a rubidium cell with single feedback mirror," Phys. Rev. Lett. **72**(15), 2379–2382 (1994).
26. C. Green, G. B. Mindlin, E. J. D'Angelo, H. G. Solari, and J. R. Tredicce, "Spontaneous symmetry breaking in a laser: The experimental side," Phys. Rev. Lett. **65**(25), 3124–3127 (1990).
27. Y. F. Chen, T. H. Lu, and K. F. Huang, "Hyperboloid structures formed by polarization singularities in coherent vector fields with longitudinal-transverse coupling," Phys. Rev. Lett. **97**(23), 233903 (2006).
28. M. P. Thirugnanasambandam, Yu. Senatsky, and K. Ueda, "Generation of very-high order Laguerre-Gaussian modes in Yb:YAG ceramic laser," Laser Phys. Lett. **7**(9), 637–643 (2010).
29. S. F. Pereira, M. B. Willemsen, M. P. van Exter, and J. P. Woerdman, "Pinning of daisy modes in optically pumped vertical-cavity surface-emitting lasers," Appl. Phys. Lett. **73**(16), 2239 (1998).
30. M. J. Padgett and J. Courtial, "Poincaré-sphere equivalent for light beams containing orbital angular momentum," Opt. Lett. **24**(7), 430–432 (1999).
31. M. Born and E. Wolf, *Principles of Optics* (Pergamon, 1980).
32. G. A. Swartzlander, Jr., "Dark-soliton prototype devices: analysis by using direct-scattering theory," Opt. Lett. **17**, 789–791 (1992).
33. Y. F. Chen and Y. P. Lan, "Dynamics of the Laguerre Gaussian TEM*0,1 mode in a solid-state laser," Phys. Rev. A **63**(6), 063807 (2001).
34. A. E. Siegman, *Lasers* (University Science, 1986).

1. Introduction

In recent decades, optical vortices (OVs) characterized by their distinct features [1] have gained increasing importance in the study of singular optics [2], light and matter interaction [1,3,4], and quantum optics [5]. Since an OV is defined as the phase singularity with vanishing intensity of a helical-phased light beam, the azimuthally circulated phase term implies the orbital angular momentum (OAM) carried by the light beam [6]. For practical interest, the characteristics associated with the OAM inspire great applications on optical tweezers [1,3,4], optical testing [7], image processing [8,9], quantum entanglement [5], and nonlinear optics [10].

Several approaches have been adopted to generate a single OV, such as mode conversions by astigmatic lenses [10,11], spiral phase plates [12], computer generated holograms [13], and optical wedges [14]. Since Hermite-Gaussian (HG) modes can be emitted by most laser cavities and are well-known eigenstates for the 2D quantum harmonic oscillator [15], via the mode conversion, a HG mode has been widely used to create a single OV [11–13] hold by a traveling-wave Laguerre Gaussian (LG) mode features azimuthally phased term $\exp(il\phi)$, where l is known as the topological charge of the vortex. The transformational relation has also been confirmed theoretically by using a Fresnel integral [16] or quantum operators connected the two complete sets of HG and LG states [17].

Aside from an isolated OV, a network of OVs can be created by means of interferometry and lead to a novel type of vortex structure. For instance, intriguing manifestations were shown corresponding to the two-dimensional (2D) optical vortex array [18] and 3D topology of optical vortex lines [19] by superposing several plane waves. Exploiting a thin-slice solid state laser [20], demonstrated the generation of vortex array beams by the interference of emitted Ince-Gaussian modes. Distinguished from an isolated OV, optical vortex array related to a network of vortices is especially useful in optical metrology [21], microlithography [22], quantum

#144024 - $15.00 USD Received 16 Mar 2011; revised 29 Apr 2011; accepted 8 May 2011; published 10 May 2011

processing [5], micro-optomechanical pumps manipulation [23], and investigating nonlinear propagation of array of singularities [24].

In this work, a novel method is carried out to produce the optical vortex array by the transformation of a standing-wave LG mode (the so-called "*flower-like*" [25] LG mode). Generation of the flower-like LG modes has been provided experimentally by utilizing a large-aperture CO2 laser [26], a solid-state laser cavity compounded of nonlinear medium [25,27,28], and a vertical-cavity surface-emitting semiconductor laser [29]. Unlike a traveling-wave LG mode, a flower-like LG mode, formed by coherent superposition of a pair of traveling-wave ones that carry the same topological charges while counter rotational wave fronts, possesses no OV and has been concerned especially in the study of pattern formation [25,27–29]. Therefore, it is fascinating and practical to raise the issue for the creation of optical vortex array by the use of the flower-like LG modes. To illustrate the feasibility, we verify firstly that a flower-like LG mode can be transformed from a set of *"crisscrossed"* HG modes theoretically. The optical vortex array is shown to be located at the cross section of the crisscrossed HG modes established by coherent superposition of a $TEM_{n,m}$ mode and a $TEM_{m,n}$ mode with well-defined relative phase α, where (n,m) designate the transverse indices in x-y directions. Since the transformational relation has been confirmed to show excellent analogy to the mode conversion of a $\pi/2$-cylindrical-lens mode converter ($\pi/2$-CLMC) [17], the investigation enables us to generate the optical vortex array experimentally by transforming the accessible flower-like LG modes through the $\pi/2$-CLMC. More importantly, adjustability of the relative phase α is qualitatively displayed in this paper by rotating the mode converter at various angles. In all, we expect the creation and exploration of the vortex light beams in our work may inspirit a more thorough study in the vortex structure and its further applications.

2. Theoretical analysis

HG modes and LG modes are complete orthonormal sets that each can well describe any amplitude distribution by an appropriate complex superposition. Besides, they are eigenmodes that can be emitted by most laser resonators. Due to comprehensive studies and accessibility of the eigenmodes, it can be understood that it is useful to create and investigate the optical vortex array by concerning those well-known eigenmodes. As a result, it may be necessary to provide firstly a brief overview of the eigenmodes and their transformational relationship.

The profile of a HG mode in terms of the Cartesian coordinates (x,y,z) with transverse indices (n,m) under paraxial approximation of the wave equation is given by [15]

$$\psi_{n,m}^{(HG)}(x,y,z)=\psi_{n,m}^{(HG)}(x,y,z)\,e^{i(n+m+1)\theta_G(z)}\;e^{-i\xi(x,y,z)}, \tag{1}$$

where

$$\psi_{n,m}^{(HG)}(x,y,z)=\frac{C_{n,m}^{(HG)}}{w(z)}\,e^{-\left(\frac{x^2+y^2}{w(z)^2}\right)}H_n\left(\frac{\sqrt{2}}{w(z)}x\right)H_m\left(\frac{\sqrt{2}}{w(z)}y\right), \tag{2}$$

with

$\xi(x,y,z)=k\,z\left[1+(x^2+y^2)/2(z^2+z_R^2)\right]$, $C_{n,m}^{(HG)}=\left(2^{n+m-1}\pi\,n!m!\right)^{-1/2}$, $w(z)=w_0\sqrt{1+(z/z_R)^2}$, w_0 is the beam radius at the waist, and $z_R=\pi w_0^2/\lambda$ is the Rayleigh range. $H_n(\cdot)$ is the Hermite polynomial of order n, k is the wave number, and $\theta_G(z)=\tan^{-1}(z/z_R)$ is the Gouy phase. Likewise, the wavefunction of a LG mode characterized by its azimuthal and radial

#144024 - $15.00 USD Received 16 Mar 2011; revised 29 Apr 2011; accepted 8 May 2011; published 10 May 2011

symmetry associated with a helical phase front $\exp(il\phi)$ can be written in terms of the cylindrical coordinates (r,ϕ,z) with radial index p and azimuthal index l as [15]

$$\psi_{p,l}^{(LG)}(r,\phi,z)=\psi_{p,l}^{(LG)}(r,\phi,z)e^{i(2p+l+1)\theta_G(z)}e^{-i\xi(r,\phi,z)}, \tag{3}$$

where

$$\psi_{p,l}^{(LG)}(r,\phi,z)=\frac{C_{p,l}^{(LG)}}{w(z)}(-1)^p\left(\frac{\sqrt{2}r}{w(z)}\right)^l L_p^l\left(\frac{2r^2}{w(z)^2}\right)e^{-\frac{r^2}{w(z)^2}}\ e^{il\phi}, \tag{4}$$

where $L_p^l(\cdot)$ is a Laguerre polynomial of azimuthal index l and radial index p, $\xi(r,\phi,z)=k\,z\left[1+r^2/2(z^2+z_R^2)\right]$, and with condition $p,l\geq 0$. Note that the azimuthal indices with different sign convention (l and $-l$) denote the equal and opposite topological charges $\pm l\hbar$ of the LG modes which implies the OAM possessed by the light beam.

Most important of all, the conversion of the Gaussian modes, which has been demonstrated and verified in detail by [16,17], can be expressed in the following with a left-right-double arrow "$\Leftrightarrow$" signifying the transformational relation

$$\psi_{p,l}^{(LG)}(r,\phi,z)\Leftrightarrow\psi_{n,m}^{(HG)}(x,y,z), \tag{5-a}$$

$$\psi_{p,-l}^{(LG)}(r,\phi,z)\Leftrightarrow\psi_{m,n}^{(HG)}(x,y,z), \tag{5-b}$$

where $p=min(n,m)$, $l=m-n$, and the relation $2p+l=n+m$ is hold for the conservation of transverse order under transformation. Explicitly, LG modes of opposite topological charges can be given by the transformation of a HG mode and its replica rotated at 90 degrees as shown in Eq. (5). To clarify the results, simplicity is added by using the Poincaré-sphere resemblance [30] since the transformation of the LG and HG modes can be well mapped on the Poincaré-sphere that has been verified to be an effective tool in dealing with the conversion of polarization states [31].

To make these formal considerations more meaningful, return to our concern of the optical vortex array. Our goal is to create a network of OVs by coherent superposition of two crisscrossed HG modes of the same order $n+m$ with a well-defined relative phase α. Hence, the wavefunction of the superposed state composed of the HG modes can straightforwardly be written as

$$\Psi_{n,m}(x,y,z,\alpha)=\psi_{n,m}^{(HG)}(x,y,z)+e^{-i\alpha}\psi_{m,n}^{(HG)}(x,y,z), \tag{6}$$

where α indicates the relative phase between the crisscrossed HG modes. An illustration for and $\alpha=\pi/2$ is shown in Fig. 1 to make Eq. (6) more clearer.

#144024 - $15.00 USD Received 16 Mar 2011; revised 29 Apr 2011; accepted 8 May 2011; published 10 May 2011

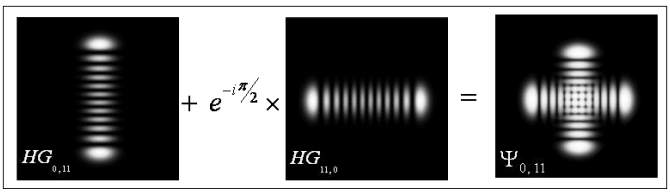

Fig. 1. Theoretical demonstration of Eq. (1) for the superposition of $\psi_{0,11}^{(HG)}$ and $\psi_{11,0}^{(HG)}$ modes with relative phase $\alpha = \pi/2$.

It is worth to mention that coherent superposition is the central concept of many quantum experiments. The phase singularities can only be arisen by coherent rather than incoherent superposition of the Gaussian modes. In [5], Alipasha Vaziri *et. al.* have emphasized the importance of preparing such superposed states for applications in quantum physics including quantum entanglement and quantum information. Though the significance of the relative phase for coherent superposition has also been appreciated in their work, a qualitative analysis and accessible experimental setup could not be seen in the research. As a result, in this article, we focus our attention on the study of the relative phase with the crisscrossed HG modes by a compact experimental configuration in order to find out its physical meaning and pivotal role in the formation of the OVs.

To determine the OVs, it should be noted that they are defined as the phase singularities where the real and imaginary components of the scalar field $\Psi_{n,m}(x,y,z,\alpha)$ are both zero and possess the characteristic of zero intensity in the vortex core [32,33]. In other words, the resulting vortices are dark points in intersects of the nodal lines corresponding to the respective HG modes of the state $\Psi_{n,m}(x,y,z,\alpha)$ with relative phase α apart from an integral multiple of π. An illustration of $\left|\Psi_{0,11}(x,y,z,\alpha)\right|^2$ is depicted in Fig. 2 with various relative phase α ranging from 0 to 2π and it can be seen the intensity distribution in the cross-section is altered accordingly. Despite this, Fig. 2 also reveals the nature that $\left|\Psi_{n,m}(x,y,z,\alpha)\right|^2$ is repeated within every period of 2π phase shift.

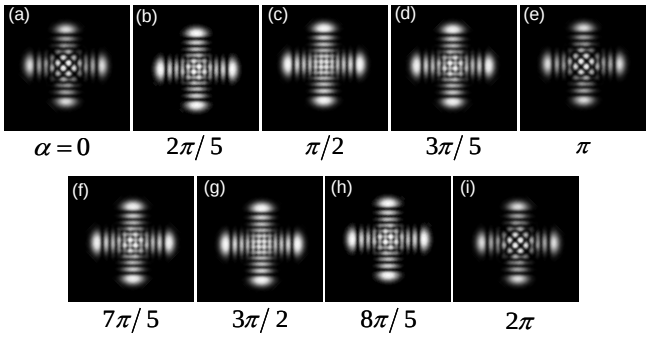

Fig. 2. Theoretical results of $\Psi_{0,11}(x,y,z,\alpha)$ of various relative phases.

For comprehensive demonstration of the vortex structure, Fig. 3 depicts the phase distribution of the state $\Psi_{0,11}(x,y,z,\pi/2)$. Though there are all 11×11 singularities which situate at the crisscrossed positions of the nodal lines as depicted in Fig. 3(b), the available OVs for practical use of particle trapping with stronger intensity distribution around [1] are estimated at in total within the cross section. The enlarged figure of the box region in Fig. 3(b) is shown in Fig. 3(c) where the black and red dots mark the vortex positions of counter rotational phase

#144024 - $15.00 USD Received 16 Mar 2011; revised 29 Apr 2011; accepted 8 May 2011; published 10 May 2011

fronts. It is conspicuously illustrated in Fig. 3(d) by plotting the transverse linear momentum density $\mathbf{p}_\perp$ of a linear polarized light beam [6]

$$\mathbf{p}_\perp = i\omega\frac{\varepsilon_0}{2}\left(\Psi^*\nabla_\perp\Psi - \Psi\nabla_\perp\Psi^*\right), \tag{7}$$

where $\mathbf{p}_\perp = \left(p_x, p_y\right)$, $\nabla_\perp = \left(\partial/\partial x\ ,\ \partial/\partial y\right)$, ω relates to the frequency of the light beam and ε_0 represents the permittivity of free space. Note that the vector field $\mathbf{p}_\perp$ has been normalized to $\mathbf{p}_\perp/\left|\mathbf{p}_\perp\right|$ for observing the detailed structures. Since the helical wave fronts signify the OAM carried by the light beam, the swirls in Fig. 3(d) shows the evidence that the superposed state $\Psi_{0,11}\left(x,y,z,\pi/2\right)$ certainly form an OAM state associated with the vortex array. From quantum perspective, preparing such superposed OAM states has become an important issue concerning quantum entanglement and quantum information [5]. Thus, it is crucial to arrange feasible experimental techniques for creating and investigating the superposed states.

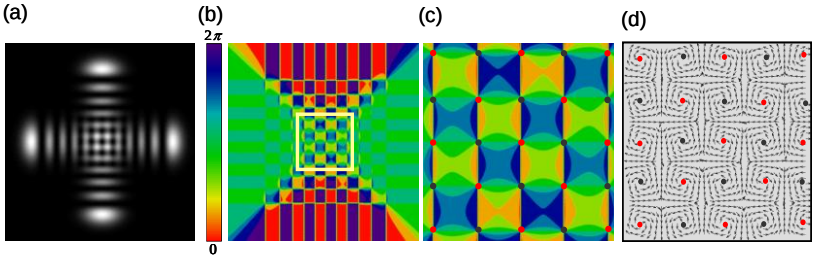

Fig. 3. (a) Theoretical results of $\Psi_{0,11}\left(x,y,z,\pi/2\right)$. (b) Phase distribution of (a). (c) Enlarged figure of the box region in (b). (d) linear momentum density $\mathbf{p}_\perp$ for the box region in (b) of $\Psi_{0,11}\left(x,y,z,\pi/2\right)$.

To develop an available experimental configuration to generate the superposed state $\Psi_{n,m}\left(x,y,z,\alpha\right)$, an inspiration is provided by the transformational relation written in Eq. (5). Likewise, we can obtain a coherent superposed state $\Phi_{p,l}\left(r,\phi,z,\alpha\right)$ according to the discussion at the very start, i.e.

$$\Psi_{n,m}\left(x,y,z,\alpha\right) \ \Leftrightarrow\ \Phi_{p,l}\left(r,\phi,z,\alpha\right) = \psi_{p,l}^{(LG)}\left(r,\phi,z,\alpha\right) + e^{-i\alpha}\psi_{p,-l}^{(LG)}\left(r,\phi,z,\alpha\right), \tag{8}$$

where, with a little algebraic manipulation, the superposed state $\Phi_{p,l}\left(r,\phi,z,\alpha\right)$ can be expressed in the form

$$\Phi_{p,l}\left(r,\phi,z,\alpha\right) = e^{-i\frac{\alpha}{2}}\frac{C_{p,l}^{(LG)}}{w(z)}(-1)^p\left(\frac{\sqrt{2}r}{w(z)}\right)^l L_p^l\left(\frac{2r^2}{w(z)^2}\right)e^{-\frac{r^2}{w(z)^2}}\times 2\cos\left[l\left(\phi+\frac{\alpha}{2l}\right)\right]. \tag{9}$$

It therefore appears that a new family of superposed state $\Phi_{p,l}\left(r,\phi,z,\alpha\right)$ is established and can be decomposed into two LG modes of opposite topological charges $\pm l$ with identical relative phase α. Compared to the traveling-wave LG mode in Eq. (4), the expression explicitly shows distinct intensity distribution of $\cos^2\left[l\left(\phi+\alpha/2l\right)\right]$ in azimuthal angle which forms the flower-like [25] LG mode of $2l$ nodes in azimuthal and possess no OAM at all. Besides, the intensity

#144024 - $15.00 USD Received 16 Mar 2011; revised 29 Apr 2011; accepted 8 May 2011; published 10 May 2011

distribution of $\Phi_{p,l}(r,\phi,z,\alpha)$ can be seen to rotate with its profile remains the same followed by the variation of as depicted in Fig. 4 of a specific case $(p,l)=(0,11)$ related to $\Psi_{0,11}(x,y,z,\alpha)$. It is worth to mention that, with the help of the arrows illustrated in Fig. 4, the state $\Phi_{0,11}(r,\phi,z,\alpha)$ is visualized obviously to rotate by an angle $\alpha/2l=2\pi/22$ through a period of 2π phase retardation. The investigation reveals the fact that the superposed state $\Psi_{n,m}(x,y,z,\alpha)$ can be repeated while the flower-like LG mode $\Phi_{p,l}(r,\phi,z,\alpha)$ rotates by $2\pi/2l$ which is exactly the angle between consecutive peaks. Experimentally, this result provides the key to qualitatively controlling the relative phase α between the crisscrossed HG modes that will be presented in the next section.

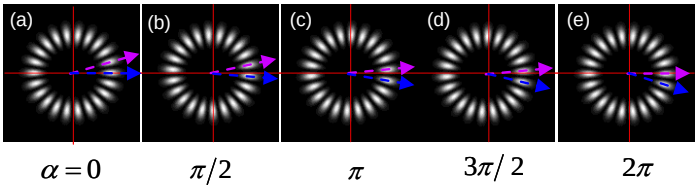

Fig. 4. Theoretical results of superposed state $\Phi_{0,11}(r,\phi,z,\alpha)$ of various relative phases.

In brief, from the theoretical point of view, the flower-like LG mode $\Phi_{p,l}(r,\phi,z,\alpha)$ has been verified to be transformed from the superposed state $\Psi_{n,m}(x,y,z,\alpha)$ composed of two crisscrossed HG modes with relative phase α. The analysis suggests the possibility that the optical vortex array can be produced effectively as long as a corresponding experimental mechanism can be found to convert an available flower-like LG mode into the crisscrossed HG mode. Thus, according to previous researches [17], which show close correspondence between the transformational relation and the mode conversion of the $\pi/2$-CLMC, we are motivated by the assertion to create the optical vortex array by transforming the flower-like LG modes via the $\pi/2$-CLMC. Markedly, different from previous works a HG mode was employed to create merely a single OV by the astigmatic lenses [10,11], the method presented in the following might improve the efficiency and effectiveness by utilizing similarly the $\pi/2$-CLMC to generate a network of vortices embedded in the superposed state.

3. Experimental results

The experimental configuration can be separated mainly into three parts according to particular purposes as depicted in Fig. 5. The microchip solid state laser cavity presented in Fig. 5(a) is utilized to generate the flower-like LG mode discussed on the above as an input mode to be transformed via the $\pi/2$-CLMC. The second part at the external cavity is consisted of a non-spherical lens and the $\pi/2$-CLMC to convert the emitted LG mode into the crisscrossed HG modes as shown in Fig. 5(b). The last part in Fig. 5(c) corresponds apparently to the detection scheme. Furthermore, detailed experimental arrangements are provided in the following.

#144024 - $15.00 USD Received 16 Mar 2011; revised 29 Apr 2011; accepted 8 May 2011; published 10 May 2011

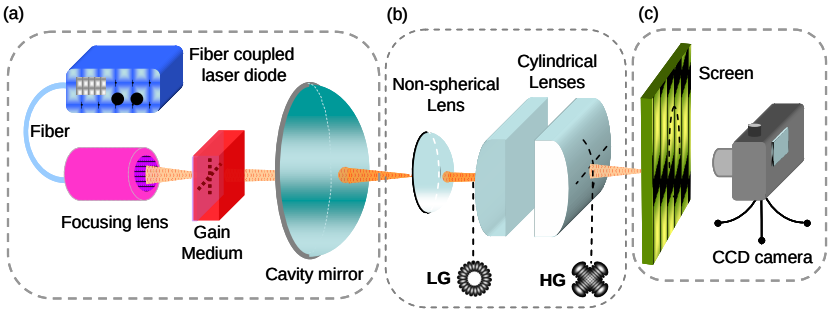

Fig. 5. Experimental setup utilized to transform the flower-like LG modes into the crisscrossed HG modes with the cylindrical lenses.

It can be seen that the laser resonator is composed of a gain medium and a spherical mirror. The laser medium is an a-cut 2.0-at. % Nd: YVO4 crystal with a length of 2 mm and the cross section 3×3 mm^2. One side of the Nd: YVO4 crystal is coated for partial reflection at 1064 nm and the other is for antireflection at 1064 nm. The radius of curvature of the cavity mirror is R = 25 cm and its reflectivity is 97% at 1064 nm. The pump source is an 808 nm fiber-coupled laser diode with pump core of 100 μm in radius, a numerical aperture of 0.16, and a maximum output power of 1 W. A focusing lens with focal length of 20 mm and 90% coupling efficiency is used to reimage the pump beam into the laser crystal. To produce a high-order flower-like LG mode, which are processed from the astigmatism and imperfection dominated by the cylindrical symmetric laser cavity, the valid key point is using a doughnut pump profile and defocusing the standard fiber-coupled diode [32,33]. The pump spot radius is controlled to be around 50-200 μm. The effective cavity length is set in the range of 1-1.5 cm. A non-spherical lens with focal length $f = 40$ mm mounted on a translation stage is exploited to provide the mode matching condition by collimating the input light beam in the midway between the following cylindrical lenses. The flower-like LG modes generated by the laser cavity are converted into the crisscrossed HG modes by passing through a rotatable -CLMC comprised of two identical cylindrical lenses with focal length $f = 25$ mm, separated by $\sqrt{2} f$. To observe the far-field pattern via a CCD camera, the output beam is directly projected to a paper screen.

According to the previous section, considering the correspondence of the transformational relation depicted in Fig. 6(a) and the mode conversion through the $\pi/2$-CLMC, we therefore utilize a rotatable $\pi/2$-CLMC to convert the accessible flower-like LG mode emitted by the laser cavity into the crisscrossed HG modes as shown in Fig. 6(b).

#144024 - $15.00 USD Received 16 Mar 2011; revised 29 Apr 2011; accepted 8 May 2011; published 10 May 2011

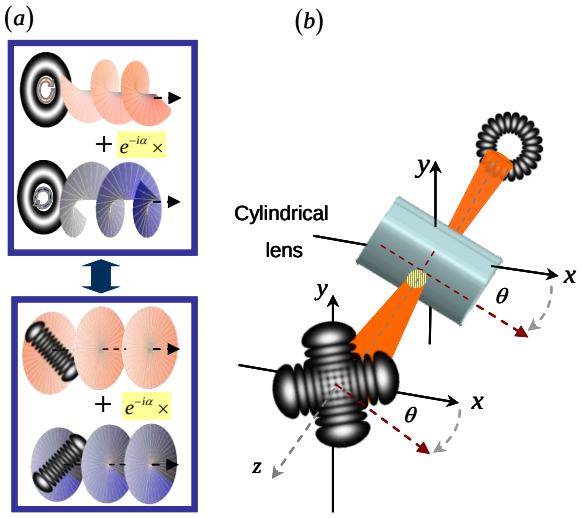

Fig. 6. (a) Diagram for the transformational relation of a flower-like LG mode and the crisscrossed HG mode. (b) Operational scheme for the rotation of the mode converter.

Because the experimental configuration is fairly stable and robust, the experimental results are reproducible and show high quality and reliability for further study and applications. Figures 7(a)–7(j) further display the experimental results of an input flower-like LG mode with $(p, l) = (0,11)$ and the corresponding output crisscrossed HG modes associated with various rotating angles θ of the $\pi/2$-CLMC. Since the output HG modes are always at 45 degrees relative to the principal axes of the cylindrical lenses, it can be seen that the crisscrossed HG modes rotate by the same angle as the mode converter. With attention to the cross section of the crisscrossed HG modes, the intensity distribution can be informed to alter accordingly with the rotating angle of the mode converter. Analogously, compared to the theoretical illustration of the superposed state $\Psi_{0,11}(x, y, z, \alpha)$ as depicted in Fig. 2, the obtained experimental results in Fig. 7(b)–7(j) are in good agreement with the theoretical realization in Fig. 2(a)–2(i) and are connected by the relation $\theta = \alpha/2l$. In essence, the manifestation of the correlation $\theta = \alpha/2l$ is none other than the geometric rotating angle of the input LG mode relative to the principal axes of the mode converter as if it was fixed. That is, the fulfillment can be understood based on our previous discussion of the superposed state $\Phi_{0,11}(r, \phi, z, \alpha)$ according to different relative phase α as shown in Fig. 4, which identically exhibits the behavior of geometric rotation by the angle $\alpha/2l$. As a result, we have successfully verified the transformational relation demonstrated in the preceding analysis by exploiting the rotatable $\pi/2$-CLMC experimentally. In other words, the optical vortex array embedded in the crisscrossed HG mode has been finally generated by the method of mode conversion with a $\pi/2$-CLMC.

#144024 - $15.00 USD Received 16 Mar 2011; revised 29 Apr 2011; accepted 8 May 2011; published 10 May 2011

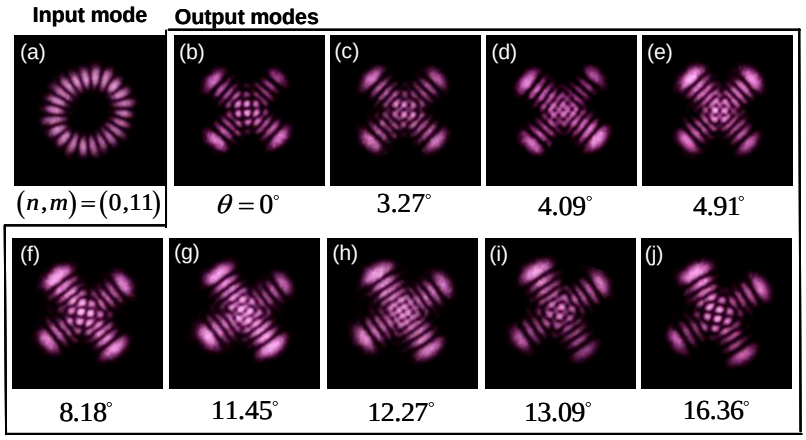

Fig. 7. Experimental results of an input LG mode with $(n,m)=(0,11)$ and the corresponding crisscrossed HG modes while rotating the CLMC.

What needs to be emphasized especially is the controllable relative phase α between the two crisscrossed HG modes, which can be qualitatively altered by rotating the $\pi/2$-CLMC at various angle. Since the relative phase has been confirmed to be the decisive factor that contributes to the formation of the phase singularities according to the above investigation, the adjustability of the relative phase in the experiment appears to be absolutely crucial to the production of the OAM state. For practical consideration, the investigation reveals the possibility of particle manipulation in two-transverse-dimension for the developing applications as it can be informed from Fig. 6(b) that the resulting vortices with fixed relative positions are simultaneously rotated with the CLMC by an angle θ. Moreover, since the Gaussian beams satisfy the property of bilinear transformation [34], which indicates that the profiles are preserved under propagation in free space through the Fourier transformation, the resulting vortex array can maintain its spatial distribution while being focused. Namely, it enables us to quantitatively determine the features of the optical vortex array that focused into the optical traps.

In addition to constructing the optical vortex array that embedded in the superposed state $\Psi_{n,m}(x,y,z,\alpha)$ with vanishing transverse index n illustrated on the above, we are now considering more complicated vortex structures determined by increasing transverse index p with multi-ring LG modes. As an illustration, Fig. 8(b) demonstrates the theoretical results of superposed states $\Psi_{1,10}(x,y,z,\pi/2)$, $\Psi_{2,10}(x,y,z,\pi/2)$, and $\Psi_{3,10}(x,y,z,\pi/2)$ with non-vanishing transverse index p corresponding to the flower-like LG modes of $\Phi_{1,9}(r,\phi,z,\pi/2)$, $\Phi_{2,8}(r,\phi,z,\pi/2)$, and $\Phi_{3,7}(r,\phi,z,\pi/2)$ as shown in Fig. 8(a). To make it clear, the associated phase distribution is demonstrated in Fig. 8(c) which explicitly shows the variation of the position of the singularities defined by the points of intersection. Since several methods have been adopted to generate the multi-ring LG modes [25–29], our investigation may provoke further application for the creation of the exotic vortex structures by transforming the available higher-order LG modes through the mode converter.

#144024 - $15.00 USD Received 16 Mar 2011; revised 29 Apr 2011; accepted 8 May 2011; published 10 May 2011

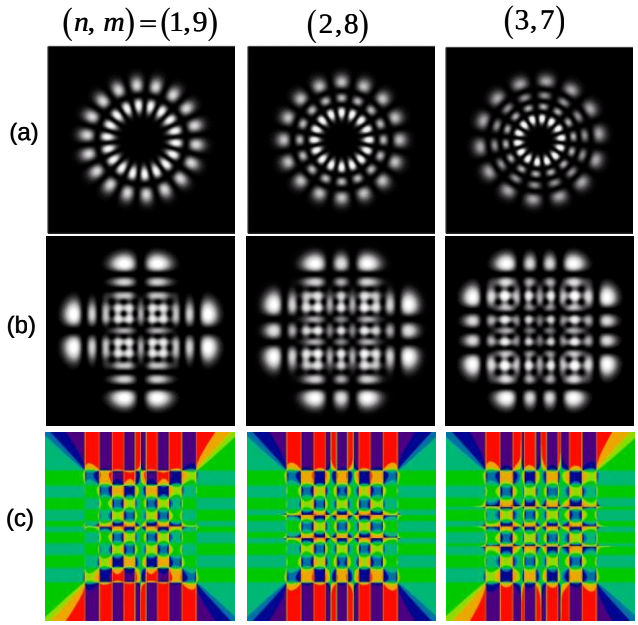

Fig. 8. Theoretical analysis: (a) LG modes with non-vanishing radial index n . (b) The resulting modes converted from the LG modes. (c) Phase distribution corresponding to (b).

4. Conclusion

In conclusion, we successfully create the optical vortex array by employing the flower-like LG modes. Theoretically, we firstly verify that the flower-like LG mode can be transformed from the crisscrossed HG modes embedded with the optical vortex array. According to excellent correspondence of the transformational relation and the mode conversion of the $\pi/2$-CLMC, we further confirm our assertion by converting the available flower-like LG modes through the $\pi/2$-CLMC. Importantly, the relative phase of the crisscrossed HG modes can be controlled qualitatively by rotating the rotatable mode converter at various angles. We anticipate the present result and method to be an inspiration for novel application and more sophisticated study related to the fascinating features of optical vortices.

Acknowledgments

The authors acknowledge the National Science Council of Taiwan (NSCT) for their financial support of this research under contract NSC96-2112-M-009-027-MY3.

#144024 - $15.00 USD Received 16 Mar 2011; revised 29 Apr 2011; accepted 8 May 2011; published 10 May 2011